

# Subnanometer confinement and bundling of atoms in a Rydberg empowered optical lattice

MOHAMMADSADEGH KHAZALI

Institute for Research in Fundamental Sciences (IPM), Tehran 19538-33511, Iran  
Department of Physics, University of Tehran, North Kargar Ave., Tehran P.O. Box 14395-547, Iran

Compiled January 12, 2023

Optical lattices are the basic blocks of atomic quantum technology. The scale and resolution of these lattices are diffraction-limited to the light wavelength. Tight confinement of single sites in conventional lattices requires excessive laser intensity which in turn suppresses the coherence due to enhanced scattering. This article proposes a new scheme for atomic optical lattice with sub-wavelength spatial structure. The potential is formed by the nonlinear optical response of the three-level Rydberg dressed atoms, which is not constrained by the diffraction limit of the driving fields. The lattice consists of a 3D array of ultra-narrow Lorentzian wells with sub-nanometer widths. The scheme allows moving adjacent sites to close distances with sub-nanometer resolution. These extreme scales are now optically accessible by a hybrid scheme deploying the dipolar interaction and optical twist of atomic eigenstates. The interaction-induced two-body resonance that forms the trapping potential, only occurs at a peculiar laser intensity, localizing the trap sites to ultra-narrow regions over the standing-wave driving field. The Lorentzian trapping potentials with 2Å width and 30MHz depth are realizable with scattering rates as low as 1Hz. The mentioned improvements allow quantum logic operations with Rydberg-Fermi interaction. These techniques are particularly demanding for the realization of atomtronics, quantum walks, Hubbard models, and neutral-atom quantum simulation. © 2023 Optical Society of America

<http://dx.doi.org/10.1364/ao.XX.XXXXXX>

## 1. INTRODUCTION

The primary enabling technology in atomic quantum processors is the coherent control of the position and motion of atoms by lasers. The underlying mechanism in conventional optical lattices is the ac-Stark shift of atomic levels formed by far-off-resonant laser fields. The diffraction limit, which is about the wavelength of the light, is what determines the scale and spatial resolution of such optical potential landscapes. This fundamentally limits the optical manipulation of atoms, affecting some of

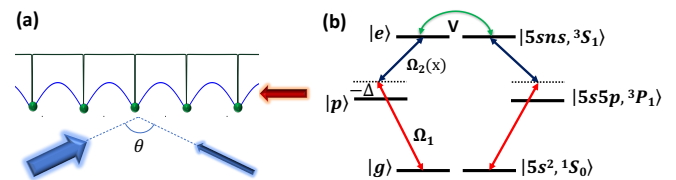


**Fig. 1.** Ultra-tight confinement of atoms in an interaction-induced atomic lattice. (a) Rydberg dressing of ground state Sr atoms with standing-wave laser field (blue line) results in an interaction-induced periodic trapping potential that features sharp resonance at a narrow range of laser intensity. This would form ultra-narrow trapping wells (green line) that results in sub-nanometer atomic confinement. (b) The level scheme presents in-resonance two-photon Rydberg excitation.

the quantum technology applications. For instance, in the recently proposed Rydberg-Fermi quantum simulator [2, 3], ultra-tight confinement of atoms within the single lobe of the Rydberg wave-function is required for high-fidelity scalable quantum processing. Tight confinement is also demanding for applications that are based on distance selective interaction [4, 5] and controlled Rydberg anti-blockade operations [6]. Finally, tight confinement is demanded for improving the fidelity of neutral atom processors [7–10].

This article presents the first scheme for ultra-tight sub-nanometer confinement of atoms in an optical lattice with dynamic features to move pair of lattice sites close to each other at extreme scales of about 4Å which is the realm of solid-state crystals. The dynamic control of the lattice separation allows a new type of quantum gate operations powered by the remote Rydberg-Fermi spin-flip. The Rydberg-Fermi spin-flip has been observed in Bose Einstein Condensate (BEC) at inter-atomic distances of about 30nm [11]. However, the real application of this phenomenon in an atomic lattice quantum processor was elusive. The real application requires dynamic maneuver of the interatomic distance from micrometer scale during the laser-addressing of individual sites [12, 13] to 30nm over the interaction stage [11]. Furthermore, since the Rydberg-Fermi interaction is proportional to the Rydberg wave-function probability amplitude, the interatomic distance must be fixed within nanometer-scale precision. The tight confinement and ultra-high precision of interatomic distances in the current lattice proposal

opens new opportunities to develop nano-scale quantum technologies of this type.

Tight confinement of atoms in conventional optical lattices requires an extensive power i.e. the spatial width is inversely proportional to the quadruple root of the laser intensity. The drawback is the loss of coherence due to the enhanced scattering. In an alternative approach, this article deploys the nonlinear response of Rydberg-dressed atoms to the intensity of standing-wave driving field, as a means to form a lattice of ultra-narrow trapping potentials. The sub-wavelength resolution arises when the composition of eigenstates on two-atom basis twists rapidly at a specific light intensity to form interaction-induced resonance over a short length scale of the standing-wave. Unlike the conventional ac-Stark shift potentials, this interaction-induced potential is a quantum effect, with magnitude proportional to  $\hbar$ . This effect forms 3D lattices with potential widths as small as the neutral atom radius. The proposed lattice features dynamic terms that bundle pairs of atoms and draw them near to sub-nanometer distances; the realm that used to be exclusive to solid state crystals.

The recent advances in optical control of Rydberg atoms have opened a wide range of applications in quantum technology [14–21]. The required dipolar interaction in this proposal is formed by the in-resonance dressing of ground-state atoms with the highly excited Rydberg state [22, 23]. Rydberg dressing of a BEC with homogeneous laser lights could form triangular and quasi-ordered droplet crystals [23, 24]. However, this periodic structure would not be fixed in space. The spatial pattern of the driving field and intensity dependence of the potential would spatially pin the lattice sites to the nodes of standing wave. Therefore, the lattice structure would be fixed in the space. This feature is required for addressing individual sites in atomic processors.

The atomic lattice *scheme* is based on dressing  $^{88}\text{Sr}$  atoms with the highly excited Rydberg level, see Fig. 1. In the two-photon in-resonance dressing scheme [22, 23], the single atom Hamiltonian is given by

$$H_i/\hbar = \frac{\Omega_1}{2}(\sigma_{gp}^i + \sigma_{pg}^i) + \frac{\Omega_2(x)}{2}(\sigma_{ep}^i + \sigma_{pe}^i) - \Delta\sigma_{pp}, \quad (1)$$

where  $\sigma_{\alpha,\beta} = |\alpha\rangle\langle\beta|$  is the transition operator. The two Rabi frequencies  $\Omega_{1,2}$  are applied by 689nm and 318nm lasers that are detuned from the intermediate state  $|p\rangle$  by  $\Delta$ . With negligible Rydberg decay rates, the system would follow the dark eigenstate  $|d\rangle \propto \Omega_2|g\rangle - \Omega_1|e\rangle$  with zero light-shift. In the limit of  $\Omega_1 \ll \Omega_2$ , ground state atoms will be partially dressed by Rydberg states with the population of  $P_e = (\Omega_1/\Omega_2)^2$ . The van-der Waals interaction between Rydberg atoms  $V_{ij} = \hbar C_6/r_{ij}^6 \sigma_{ee}^i \sigma_{ee}^j$  is a function of interatomic distance  $r_{ij}$ . The interaction of  $[5sns^3S_1]$  Rydberg atoms is repulsive. This strong interaction could exceed atom-light coupling over several micrometers of interatomic separations.

The dynamic of the system under Rydberg interaction is governed by the master equation of two-body density matrices. The two-body density matrices  $\rho_{ij} = \text{Tr}_{i,j}\rho$  are obtained by tracing over all but  $i$  and  $j$  particles. The corresponding master equation would be given by

$$\partial_t \rho_{ij} = -\frac{i}{\hbar}[H_i + H_j + V_{ij}, \rho_{ij}] + \mathcal{L}_i(\rho_{ij}) + \mathcal{L}_j(\rho_{ij}) \quad (2)$$

The internal state dynamics are governed by single-particle dissipation described by  $\mathcal{L}_i$  operator acting on  $i$ th atom. The Liouvillian term  $\mathcal{L}_i(\rho) = \sum_{\beta} \mathcal{D}(c_{\beta})\rho_i$  with  $\mathcal{D}(c)\rho_i = c\rho_i c^\dagger - 1/2(c^\dagger c\rho_i +$

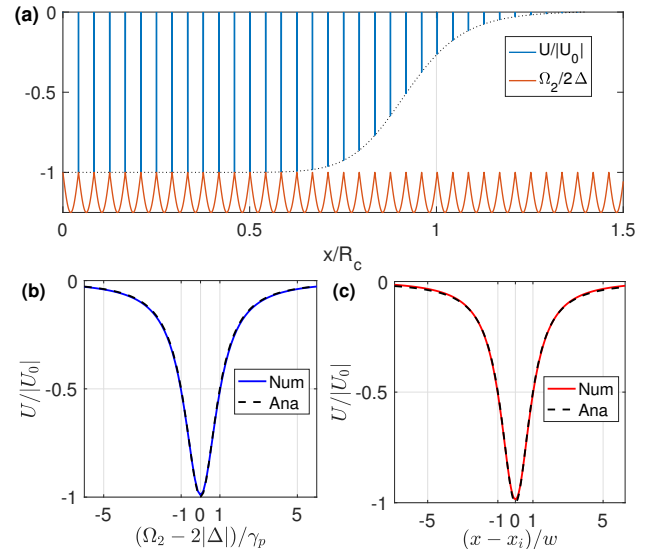


**Fig. 2.** Interaction-induced atomic lattice. (a) The red line shows the spatial profile of the Rabi frequency  $\Omega_2(x) = \Omega_{2c} + \Omega_{2sw} |\sin(kx \sin(\theta/2))|$ , where  $k = 2\pi/\lambda$ . The blue line shows the interaction of two atoms as a function of interatomic distance. When two atoms are within the soft-core radius and are both located at the nodes of the standing wave they experience a strong trapping potential. With a single atom per lattice site, the effective trapping interaction would be the sum of two-body interactions of all the sites within the  $\pm R_c$  distance. (b) The interaction induced resonance occurs at  $\Omega_2 = 2|\Delta|$ , with maximum depth of  $U_0 = \frac{3\hbar\Omega_1^4}{8\Delta\gamma^2}$  and a HWHM of  $\Omega_2 - 2|\Delta| = \pm\gamma_p$ . The analytical form of Eq. 5 and numerical calculation of the interaction potential (Eq. 3) presents a perfect match. (c) Spatial form of the interaction-induced trap at the position of the  $i$ -th standing wave node. The Lorentzian potential of Eq. 6 with the width  $w$  (Eq. 7) shows a perfect match with the numeric calculation of Eq. 3. Chosen parameters in (a) are  $\Omega_{2c} = 2\Delta = 2\pi \times 10\text{MHz}$ ,  $\Omega_{2sw} = \Delta/2$  loss limited to 1Hz,  $n = 100$ ,  $\theta = \pi$ .

$\rho_i c^\dagger c$ ) in the Lindblad form governs the dissipative time evolution. Lindblad terms encounter spontaneous emission from Rydberg  $c_{pe} = \sqrt{\gamma_e}|p\rangle\langle e|$  and intermediate level  $c_{gp} = \sqrt{\gamma_p}|g\rangle\langle p|$ . The spontaneous emission rates are  $\gamma_p/2\pi = 7.6\text{kHz}$  and  $\gamma_e$  can be found in [25].

Considering the steady state  $\bar{\rho}_{ij}$  of Eq. 2, the effective interaction would be given by

$$U(r_{ij}) = \text{Tr}[\bar{\rho}_{ij}(H_i + H_j + V_{ij})]. \quad (3)$$

For homogeneous lasers, a plateau-type interaction profile would be formed with constant interaction within the soft-core as depicted by the dotted line in Fig. 2a. In Rydberg-dressing the interaction region is defined by  $R_c$ ; the interatomic distance within which interaction-induced laser detuning equals the effective laser bandwidth  $P_r V(R_c) = \Omega_1 \Omega_2 / 2\Delta$  [23]. The soft-core interaction features a sharp peak at  $\Omega_2 = 2|\Delta|$ , due to an interaction-induced resonance, see Fig. 2b.

To form the optical lattice with the mentioned interaction-induced resonance, a space-dependent variation of the upper laser is deployed. Using different intensities for the counter-propagating 318nm lasers, results in the desired spatial pattern

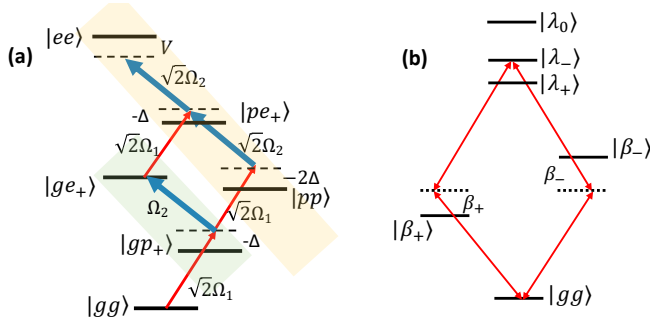


**Fig. 3.** The origin of the trapping potential is the interaction-induced resonance at  $\Omega_2 = 2|\Delta|$ . (a) With  $\Omega_1 \ll \Omega_2$  the two-atom Hilbert space would be organized in three subspaces of ground state, single-excitation (green box) and double-excitations (yellow box) that are coupled by weak  $\Omega_1$  laser. (b) The effects of strong coupling  $\Omega_2$  and interaction  $V$  could be observed by diagonalizing the green and yellow subspaces with eigen-states of  $|\beta_{\pm}\rangle$  and  $|\lambda_{0,\pm}\rangle$  respectively. At the nodes of the standing wave  $\Omega_2(x) = -2\Delta$ , the interaction-induced level shift, makes the  $|\lambda_{-}\rangle$  in-resonance with the ground state, significantly enhancing the interaction and forming the trapping potential.

of the Rabi frequency

$$\Omega_2(x) = \Omega_{2c} + \Omega_{2sw} |\sin(kx \sin(\theta/2))|, \quad (4)$$

where  $k = 2\pi/\lambda$  is the laser wave-vector and  $\theta$  is the angle between counter propagating lights, see Fig. 1a. Adjusting  $\Omega_{2c} = -2\Delta$  in Eq. 4 forms periodic trapping potentials at the nodes of standing wave upon the presence of at least two atoms within the core radius  $R_c$ , see Fig. 2a,c. In a 1D lattice with single atom occupation per site, the effective potential experienced by each site is the sum of two-body interactions of neighboring lattice sites within the interacting range of  $\pm R_c$ . Considering the isotropic Rydberg interaction of the  $S$  orbital, extension to the 3D lattice is trivial.

Here we analytically formulate the interaction-induced resonance peak around  $\Omega_2(x) = 2|\Delta|$ . Considering the level scheme of Fig. 3a in two-atom basis, the doubly excited Rydberg state asymptotically decouples within the interaction region  $R_c$  as  $V \rightarrow \infty$ . Taking into account the remaining states, in the limit of  $\Omega_1 \ll \Omega_{2c}$  the steady state density could be obtained by adding three orders of perturbative corrections to the initial ground state. In the limit of  $\gamma_p \ll \Delta$  the dressing interaction of the steady state simplifies to

$$U(x) = \frac{\hbar\Omega_1^4}{\Omega_2(x)^2} \frac{4\Delta[2\Delta^2 + \Omega_2(x)^2]}{[4\Delta^2 - \Omega_2(x)^2]^2 + 16\gamma_p^2\Delta^2}. \quad (5)$$

The maximum interaction occurs at  $\Omega_2 = 2|\Delta|$  with the value of  $U_0 = \frac{3\hbar\Omega_1^4}{8\Delta\gamma_p^2}$ . Note that the attractive or repulsive nature of the potential peak is determined by the sign of detuning  $\Delta$ . The half-width at half-maximum of interaction peak occurs at  $\Omega_2(x) - 2|\Delta| = \pm\gamma_p$ . The presented analytic model of Eq. 5 perfectly resemble the numerical results, see Fig. 2. Considering the spatial variation of the  $\Omega_2$  in Eq. 4 over the narrow area of the potential peak  $k \cdot (x - x_i) \ll 1$  with  $\Omega_{2c} = -2\Delta$ , the spatial profile of the  $i^{\text{th}}$  trapping site has a Lorentzian form

$$U_i(x) = \frac{U_0}{1 + (x - x_i)^2/w^2} \quad (6)$$

where the half-width at half-maximum and the depth of the spatial trap well are given by

$$w = \frac{\gamma_p}{k \sin(\theta/2) \Omega_{2sw}}; \quad U_0 = \frac{3\hbar\Omega_1^4}{8\Delta\gamma_p^2}. \quad (7)$$

Figure 2c compares this analytical form of Eq. 6 with the numerical results. The scale of the trap width as a function of  $\Omega_{2sw}$  is plotted in Fig. 4c. Remarkably, with  $\Omega_{2sw}/2\pi = 1.7\text{MHz}$  the trap width would be as tight as the radius of  $^{88}\text{Sr}$  atoms.

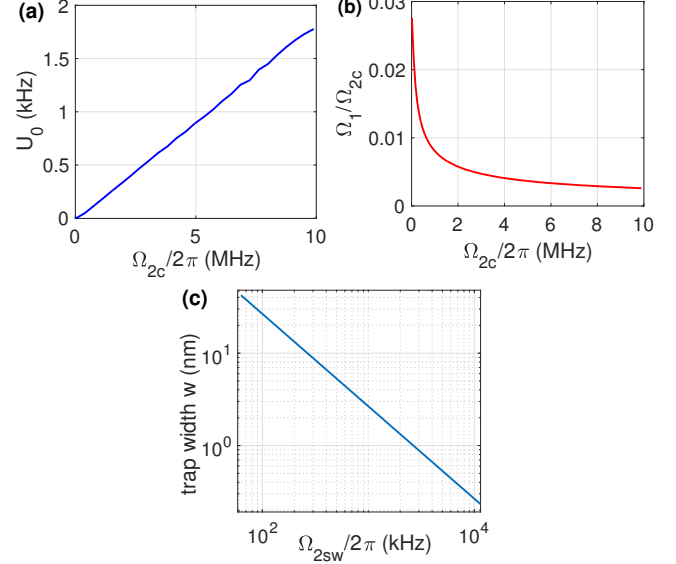


**Fig. 4.** (a) The scale of trap depth  $U_0$  for two atoms located within the core distance of  $R_c$  is plotted as a function of  $\Omega_{2c}$  for the constant scattering rate of 1Hz. Having  $N$  lattice sites within the interaction distance  $R_c$ , the trapping potential experienced by an atom would add up to  $NU_0$ . (b) The decoherence rate is adjusted to 1Hz by controlling the ratio of  $\Omega_1/\Omega_{2c}$ . (c) The width of Lorentzian traps  $w$  (Eq. 7) is plotted as a function of  $\Omega_{2sw}$  for  $\theta = \pi$ .

The origin of the enhanced interaction at  $\Omega_2 = 2|\Delta|$  can be traced to two-atom resonance that occurs in the presence of strong interaction [22]. Considering the laser coupling on the two-atom basis, for  $\Omega_1 \ll \Omega_2$  the two-atom Hilbert space would be organized in three subspaces that are coupled by weak  $\Omega_1$  laser, see Fig. 3. These subspaces are the ground state  $|gg\rangle$ , one atom excitation  $\{|gp\rangle_+, |ge\rangle_+\}$ , and two atom excitation states  $\{|pp\rangle, |pe\rangle_+, |ee\rangle\}$ , with  $|\alpha\beta\rangle_+ = (|\alpha\rangle + |\beta\rangle)/\sqrt{2}$  represents symmetric two-particle states. The strong coupling  $\Omega_2$ , mixes the states in each subspace. Pre-diagonalizing the subsystems quantifies the light-shifts experienced by the eigen-states, see Fig. 3b. For the second subspace with single excitation, the coupling Hamiltonian in the  $\{|gp\rangle_+, |ge\rangle_+\}$  basis is given by

$$S_2/\hbar = \begin{pmatrix} -\Delta & \Omega_2/2 \\ \Omega_2/2 & 0 \end{pmatrix}. \quad (8)$$

The eigen-energies in this subspace  $\beta_{\pm}/\hbar = -\Delta/2 \pm 1/2\sqrt{\Delta^2 + \Omega_2^2}$  does not get resonant with the ground state. In the third subspace with double excitations, the coupling Hamil-

tonian in the  $\{|pp\rangle, |pe\rangle_+, |ee\rangle\}$  basis is given by

$$S_3/\hbar = \begin{pmatrix} -2\Delta & \Omega_2/\sqrt{2} & 0 \\ \Omega_2/\sqrt{2} & -\Delta & \Omega_2/\sqrt{2} \\ 0 & \Omega_2/\sqrt{2} & V \end{pmatrix}. \quad (9)$$

For large interaction inside the softcore  $V \rightarrow \infty$ , the eigen-energies are  $\lambda_0 = V$  and  $\lambda_{\pm} = -\frac{3\hbar}{2}\Delta \pm \hbar/2\sqrt{\Delta^2 + 2\Omega_2^2}$ . The doubly excited Rydberg state  $|\lambda_0\rangle \approx |ee\rangle$  decouples asymptotically. At  $\Omega_2 = 2|\Delta|$  one of  $|\lambda_{\pm}\rangle$  eigen-states couples resonantly with the ground state, generating an enhanced light-shift. As discussed above, small deviation of laser intensity  $\Omega_2 - 2|\Delta| = \pm\gamma_p$  makes the  $\lambda_-$  eigen-state out of resonance. Hence, the interaction-induced resonant peaks would be localized at very narrow areas of the  $\Omega_2(x)$  standing-wave.

The main source of *decoherence* in this system is the spontaneous emission from the intermediate state. Rydberg interaction disturbs individual atom's dark state, populating the intermediate state  $|p\rangle$ , and hence increases the loss rate per atom  $\Gamma = \text{Tr}[\rho_i(\gamma_p\sigma_{pp} + \gamma_e\sigma_{ee})]$  at the trapping potential teeth. The loss rate spatial profile is approximately given by  $\gamma_p U(x)/\Delta$ . The maximum loss for a given  $\Omega_2(x)$  profile could be controlled by adjusting the intensity of  $\Omega_1$  laser. The scale of trap depth for two atoms located within the soft-core is plotted in Fig. 4a as a function of  $\Omega_{2c}$  for the constant scattering rate of 1Hz. The interaction-to-loss ratio enhances by applying stronger laser driving of  $\Omega_{2c}$ . Having  $N$  single-atom-occupied trapping sites within the  $\pm R_c$  interaction distance, the trapping potential experienced by an atom would add up to  $NU_0$ . In a case study, considering the lattice constant of  $\lambda/2$ , dressing ground state atoms to  $|5s100s^3S_1\rangle$  with  $\Omega_{2c}/2\pi = 10\text{MHz}$  and limiting the loss rate to 1Hz, the collective trapping potential experienced by a single atom in 1D (3D) lattice interacting by neighboring sites within the soft-core would be  $N_{1D}U_0 = 77\text{kHz}$ , ( $N_{3D}U_0=37\text{MHz}$ ).

An important feature of the proposed Rydberg-empowered optical lattice is the possibility to move the pair lattice sites close to each other by manipulating the laser intensity. The inter-atomic distance could approach the extreme scales that used to be limited to solid-state crystals. As mentioned above, the resonance trapping potential occurs at the points of standing waves that fulfill the  $\Omega_{2c} + \Omega_{2sw}|\sin(kx \sin(\theta/2))| = 2|\Delta|$ . Accordingly, by adjusting the  $\Omega_{2c}$  and  $\Omega_{2sw}$  the resonance could occur at positions other than the nodes of the standing-wave driving-field, making a lattice of dimers as shown in Fig. 5b. To find the precision in adjusting the minimum interatomic distance, consider the case that the pair sites are very close to the position of the nodes  $|x - x_n| \ll (k \sin(\theta/2))^{-1}$  where  $x_n$  is the position of a random node. At this regime, the separation of two lattice sites from a node would be given by  $x - x_n = \pm(2|\Delta| - \Omega_{2c})/(\Omega_{2sw}k \sin(\theta/2))$ . Therefore, having larger  $\Omega_{2sw}$  would enhance the adjustment precision of intradimer lattice spacing. A sample laser parameters for trapping two lattice sites at  $4\text{\AA}$  distance are  $\Omega_{2sw}/2\pi = 10\text{MHz}$  and  $2|\Delta| - \Omega_{2c} = 2\pi \times 25\text{kHz}$  and  $\theta = \pi$  which are experimentally realizable.

**Outlook-** The sub-nanoscale resolution in trapping and bundling of pair sites demonstrated here extends the toolbox of neutral atom quantum technology. Ultra-narrow wells in this proposal allow significant suppression of the lattice constant with a time-sharing approach [26]. In this approach, the applied standing wave is stroboscopically shifted in space by  $\lambda/2N$  and

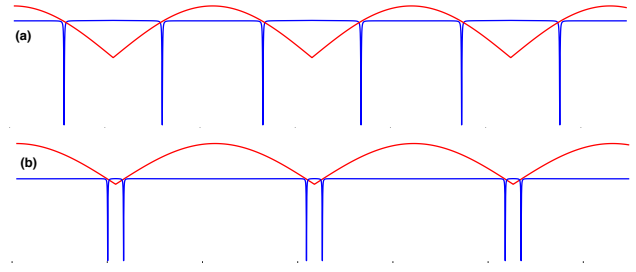


**Fig. 5.** Moving lattice sites by adjusting the relative intensity of counter-propagating lasers. The lattice constant is originally  $\Lambda/4$  in (a). By changing the laser intensity, the resonance condition  $\Omega_2(x) = 2|\Delta|$  fulfills at positions other than the nodes of standing-wave, forming a lattice of dimers. The distance of the atomic pairs could be made as small as  $4\text{\AA}$ .

hence the effective lattice constant would be smaller by a factor of  $N^{-1}$ . This compaction of the atomic lattice is quite demanding for scaling the lattice sites with the current limited laser powers. Furthermore, in quantum simulation with optical lattices, the energy scale of Hubbard models for both hopping and interaction of atoms is set by the minimum lattice constant which used to be limited to  $\lambda/2$ , leading to challenging temperature requirements to observe quantum phases of interest [1].

A distinct research avenue looks at the applications of the presented scheme with ultra-narrow repulsive peaks. Equation 5 shows that changing the detuning sign would preserve the interaction profile but only flip the potential sign from attractive to repulsive. These ultra-narrow barriers are ideal for the realization of the Kronig-Penney (KP) lattice model [27]. Furthermore, the three dimensional repulsive  $\delta$ -function peaks form nearly perfect box-traps [28]. These repulsive narrow peaks also realize thin tunnel junctions for atomtronic devices [29, 30]. The potential is easily generalizable to other geometries in three dimensions using the holographically designed laser intensity [31].

## REFERENCES

1. C. Gross and I. Bloch, *Science* **357**, 995 (2017).
2. M Khazali, W Lechner, Electron cloud design for Rydberg multi-qubit gates, arXiv:2111.01581 (2021).
3. Khazali, Mohammadsadegh, Universal terminal for mobile edge-quantum computing, arXiv:2204.08522 (2022).
4. M. Khazali, ?Discrete-Time Quantum-Walk & Floquet Topological Insulators via Distance-Selective Rydberg-Interaction?, *Quantum* **6**, 664 (2022).
5. Hollerith, S., Srakaew, K., Wei, D., Rubio-Abadal, A., Adler, D., Weckesser, P., Kruckenhauser, A., Walther, V., van Bijnen, R., Rui, J. and Gross, C., Realizing distance-selective interactions in a Rydberg-dressed atom array. *Phys. Rev. Lett.*, **128**, 113602 (2022).
6. C. Ates, T. Pohl, T. Pattard, and J. M. Rost, "Antiblockade in Rydberg excitation of an ultracold lattice gas." *Phys. Rev. Lett.* **98**, 023002 (2007).
7. Graham, T.M., Kwon, M., Grinkemeyer, B., Marra, Z., Jiang, X., Lichtman, M.T., Sun, Y., Ebert, M. and Saffman, M., Rydberg-mediated entanglement in a two-dimensional neutral atom qubit array. *Phys. Rev. Lett.*, **123**, 230501 (2019).
8. A. Pagano, S. Weber, D. Jaschke, T. Pfau, F. Meinert, S. Montangero, and H. P. Büchler, Error budgeting for a controlled-phase gate with strontium-88 Rydberg atoms, *Phys. Rev. Research* **4**, 033019 (2022).
9. Cetina, M., Egan, L.N., Noel, C., Goldman, M.L., Biswas, D., Risinger, A.R., Zhu, D. and Monroe, C., Control of transverse motion for quan-

- tum gates on individually addressed atomic qubits. *PRX Quantum*, **3**, 010334 (2022).
10. Brennen, G.K., Caves, C.M., Jessen, P.S. and Deutsch, I.H., Quantum logic gates in optical lattices. *Phys. Rev. Lett.* **82**, 1060 (1999).
  11. Niederprüm, T., Thomas, O., Eichert, T., and Ott, H. Rydberg molecule-induced remote spin flips. *Phys. Rev. Lett.* **117**, 123002 (2016).
  12. C. Weitenberg, M. Endres, J. F. Sherson, M. Cheneau, P. Schauß, T. Fukuhara, I. Bloch & S. Kuhr, "Single-spin addressing in an atomic Mott insulator." *Nature* **471** 319 (2011).
  13. M. Saffman, "Quantum computing with atomic qubits and Rydberg interactions: progress and challenges." *J. Phys. B* **49**, 202001 (2016).
  14. M. Saffman, T. G. Walker, and K. Mølmer. "Quantum information with Rydberg atoms." *Rev. Mod. Phys.* **82**, 2313 (2010).
  15. M. Khazali and K. Mølmer. Fast multiqubit gates by adiabatic evolution in interacting excited-state manifolds of rydberg atoms and superconducting circuits. *Phys. Rev. X*, **10**, 021054, (2020).
  16. M. Khazali, C. R Murray, and T. Pohl. Polariton exchange interactions in multichannel optical networks. *Physical Review Letters*, **123** 113605, 2019.
  17. M. Khazali, K. Heshami, and C. Simon. Photon-photon gate via the interaction between two collective Rydberg excitations. *Physical Review A*, **91** 030301, (2015).
  18. M. Khazali, All optical quantum information processing via a single-step Rydberg blockade gate, arXiv:2211.06998 (2022)
  19. M. Khazali, K. Heshami, and C. Simon. Single-photon source based on Rydberg exciton blockade. *J. Phys. B: At. Mol. Opt. Phys.*, **50**, 215301, (2017).
  20. M. Khazali, H. W. Lau, A. Humeniuk, and C. Simon. Large energy superpositions via Rydberg dressing. *Phys. Rev. A*, **94**, 023408, (2016); M. Khazali. Progress towards macroscopic spin and mechanical superposition via Rydberg interaction. *Phys. Rev. A*, **98**, 043836, (2018).
  21. M. Khazali, "Quantum information and computation with Rydberg atoms." *Iranian Journal of Applied Physics* **10** 19 (2021); M. Khazali, Applications of Atomic Ensembles for Photonic Quantum Information Processing and Fundamental Tests of Quantum Physics. Diss. University of Calgary (Canada), (2016).
  22. C. Gaul, B. J. DeSalvo, J. A. Aman, F. B. Dunning, T. C. Killian, and T. Pohl, Resonant Rydberg Dressing of Alkaline-Earth Atoms via Electromagnetically Induced Transparency, *Phys. Rev. Lett.* **116**, 243001 (2016).
  23. M. Khazali, Rydberg noisy dressing and applications in making soliton molecules and droplet quasicrystals, *Phys. Rev. Research* **3**, L032033 (2021)
  24. Henkel, N., Cinti, F., Jain, P., Pupillo, G. and Pohl, T., Supersolid vortex crystals in Rydberg-dressed Bose-Einstein condensates. *Physical Review Letters* **108**, 265301 (2012).
  25. S. Kunze, R. Hohmann, H. J. Kluge, J. Lantzsch, L. Monz, J. Stenner, K. Stratmann, K. Wendt, and K. Zimmer, Lifetime measurements of highly excited Rydberg states of strontium I, *Z. Phys. D* **27**, 111 (1993).
  26. S. Nascimbene, N. Goldman, N. R. Cooper, and J. Dalibard, Dynamic optical lattices of sub-wavelength spacing for ultracold atoms, *Phys. Rev. Lett.* **115**, 140401 (2015).
  27. R. de L. Kronig and W. G. Penney, *Proc. Roy. Soc. A* **130**, 499 (1931).
  28. A. L. Gaunt, T. F. Schmidutz, I. Gotlibovych, R. P. Smith, and Z. Hadzibabic, Bose-Einstein condensation of atoms in a uniform potential, *Phys. Rev. Lett.* **110**, 200406 (2013).
  29. BT. Seaman, M. Krämer, DZ. Anderson, MJ. Holland, "Atomtronics: Ultracold-atom analogs of electronic devices." *Physical Review A* **75.2** (2007): 023615.
  30. S. Eckel, J. G. Lee, F. Jendrzejewski, N. Murray, C. W. Clark, C. J. Lobb, W. D. Phillips, M. Edwards, and G. K. Campbell, Hysteresis in a quantized superfluid atomtronic circuit, *Nature* **506**, 200 (2014).
  31. Barredo, D., Lienhard, V., De Leseleuc, S., Lahaye, T. and Browaeys, A., Synthetic three-dimensional atomic structures assembled atom by atom. *Nature* **561**, 79 (2018).